Contractile units in disordered actomyosin bundles arise from F-actin buckling — Supplement: Non-identical motor spacings and force-dependent filament detachment

The model presented in the main text is designed to be as simple as possible while accounting for experimental observations. Namely, we demand that it recapitulate bundle contractility at relatively high myosin concentration, and the absence of contractility at low myosin density. This requires including non-identical motor unloaded velocities and motor detachment in the model. While these simple features yield good agreement with the experiments, one might wonder how additional features of realistic systems would affect our conclusions. Here we numerically investigate two such features: a distribution of inter-motor distances ℓ_0 and the dependence of the motor detachment rate on applied force. We find that neither significantly affects our main results, which confirms that the simple model of the main text captures the essential physics of the system studied.

We solve Eqs. (1-4) of the main text numerically with finite but small $\mathrm{d}t$ for an array of $N = 10$ motors and including the effects of motor detachment. If the motor stall forces are all identical (*i.e.*, $\delta F_S = 0$), force buildup within the bundle does not occur, thus preventing contraction. Instead, we choose the motor stall forces at random from a distribution with significant spread, *i.e.*, one whose standard deviation is comparable to its mean. We thus pick stall forces from a homogeneous distribution between 0 and $2F_S$ (thus $\delta F_S = F_S/\sqrt{3}$). We do not expect our results to strongly depend on the precise form of this distribution. We start the simulations with a relaxed bundle ($f_i = 0$) and run them long enough to reach a steady state for $\sum_{i=1}^{N} f_i^2$. Here we present results for $f_\infty^2 = \lim_{t\to\infty} \overline{\langle f^2 \rangle}$. All values of f_∞ presented here are averaged over 100 independent realizations of the system, each with a different set of motor stall forces, as well as motor spacings when appropriate. The steady-state force in each realization is averaged over time after the simulation reaches its steady state.

To study the effect of a distribution of inter-motor distances ℓ_0, we compare the case where $\ell_0 = \ell_0^{\mathrm{avg}}$ everywhere with a situation where ℓ_0 is homogeneously distributed in the interval

$$\ell_0^{\mathrm{avg}}/2 < \ell_0 < 3\ell_0^{\mathrm{avg}}/2. \tag{S1}$$

This distribution is chosen for its significant spread and the fact that it avoids numerical convergence issues due to very small values of ℓ_0. Again, we do not expect our results to strongly depend on the precise form of this distribution. As shown by the dashed line in Fig. S1, we find that the relationship between the steady state force f_∞ and the motor detachment time τ_d is qualitatively similar to that given by the analytical solution

$$f_\infty = \frac{1}{2\sqrt{3}} \left(\frac{\ell_f}{\ell_0}\right)^{1/2} \frac{\delta F_S}{1 + \tau_r/\tau_d} \tag{S2}$$

given in the main text (see Fig. S1, solid line). The distribution of ℓ_0 results in a horizontal shift of the curve by a factor of order one, an effect that is unimportant for the scaling analysis of the main text.

To study the effect of force-dependent motor detachment, we assume that the rate of motor detachment depends on the force exerted by the filament on the motor. Experiments performed with smooth muscle myosin indicate that a motor detaches less frequently (more frequently) when the exerted force opposes (assists) its natural motion, a tendency known as the Fenn effect [1]. These observations suggest an exponential dependence for the rate of detachment of motor i:

$$\frac{1}{\tau_d} \exp\left(\frac{f_i - f_{i-1}}{f_d}\right) \tag{S3}$$

As shown in the inset of Fig. S1, this dependence involves a typical force $f_d \simeq 2.8\,\mathrm{pN}$. We plot the resulting dependence of the typical filament force f_∞ on the dimensionless unloaded detachment rate τ_r/τ_d for different

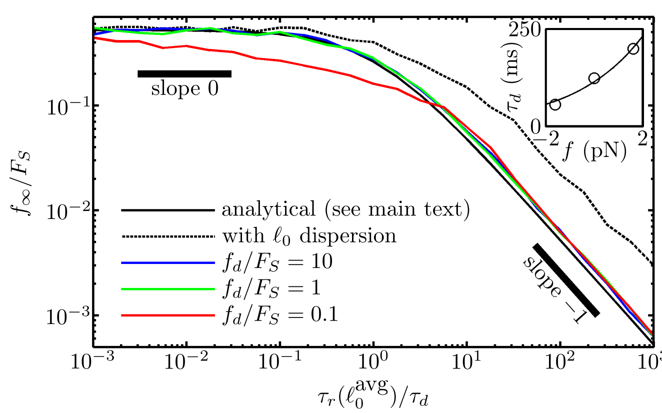

FIG. S1. Effect of inhomogeneous inter-motor spacings and force-dependent motor detachment on the steady-state filament force. The typical steady-state filament force f_∞ is plotted as a function of the dimensionless unloaded detachment rate τ_r/τ_d. Two asymptotic behaviors identical to those apparent in Fig. 4 of the main text are observed. Little difference is observed between the calculation of the main text [*solid black line*—Eq. (S2)], the case with inhomogeneous inter-motor spacing ℓ_0 [*dashed line*—see Eq. (S1)], and the case with force-dependent motor detachment [*colored lines*—see Eq. (S3)]. *Inset:* Fit of the relationship Eq. (S3) to the data of Ref. [1] (*circles*), yielding $f_d \simeq 2.8\,\mathrm{pN}$.

values of f_d in Fig. S1. Since f_d and F_S are both expected to be $\approx$pN, we show three curves covering the range of realistic ratios $f_d/F_S = 10$, 1 and 0.1. The two first curves are found to be very close to the result of the main text (corresponding to $f_d = \infty$), while third one differs from it by a factor of order one at most.

Taken together, the results of this section indicate that neither a distribution of inter-motor spacing nor a force-dependent detachment rate have a strong influence on the results presented in the main text. This thus validates our simplifying assumptions of constant ℓ_0 and τ_d in the frame in our scaling/order-of-magnitude approach.

[1] Claudia Veigel, Justin E Molloy, Stephan Schmitz, and John Kendrick-Jones. Load-dependent kinetics of force production by smooth muscle myosin measured with optical tweezers. *Nat. Cell Biol.*, 5(11):980–986, November 2003.